Available online at www.sciencedirect.com

SciVerse ScienceDirect

Energy Procedia

ELSEVIER

Energy Procedia 33 (2013) 186 – 197

PV Asia Pacific Conference 2012

An Investigation on Structural and Electrical Properties of RF-Sputtered Molybdenum Thin Film Deposited on Different Substrates

N. Dhar[a], P. Chelvanathan[a], M. Zaman[b], K. Sopian[a], N. Amin[a,b,c*]

[a]*Solar Energy Research Institute, The National University of Malaysia, 43600 Bangi, Selangor, Malaysia*
[b]*Department of Electrical, Electronic and System Engineering, Faculty of Engineering and Built Environment, The National University of Malaysia, 43600 Bangi, Selangor, Malaysia*
[c]*Center of Excellence for Research in Engineering Materials (CEREM), College of Engineering, King Saud University, Riyadh 11421, Saudi Arabia*

Abstract

Molybdenum (Mo) is the prominent choice as the back contact for various thin film solar cells such as CIGS, CZTS and CdTe. Physical vapour deposition (PVD) technique especially sputtering process has been chosen as the foremost method to deposit Mo thin film on top of desired substrate due to ease of parametric control of growth conditions. In this paper, we reported the effect of various RF power, operating pressure as well as temperature on Mo films on top of Mo sheet and soda lime glass (SLG) deposited using RF magnetron sputtering. Uniform surface morphology was obtained as RF power, operating pressure and deposition temperature were optimised. However, at higher deposition temperature less uniform surface was observed. XRD pattern of Mo films showed two different peak of <200> and <211> in case of Mo sheet and single peak <110> in case of SLG. While peak intensity varies as deposition condition varies in case of Mo films deposited on Mo sheet. Electrical properties of Mo films on both Mo sheet and SLG were improved as RF power and deposition temperature are optimised. On the other hand, electrical properties are affected as operating pressure increased. Lower resistivity of 1.2×10^{-9} Ω.m and 6.65×10^{-6} Ω.m were found in case of Mo films deposited on Mo sheet and SLG. Surface roughness of 0.017 nm-19.32 nm were found in case of Mo films deposited on Mo sheet and 0.002 nm-5.04 nm were found in case of SLG. Roughness increased as RF power and deposition temperature increased. However, roughness decreased as operating pressure increased.

© 2013 The Authors. Published by Elsevier Ltd. Open access under CC BY-NC-ND license.
Selection and peer-review under responsibility of Solar Energy Research Institute of Singapore (SERIS) – National University of Singapore (NUS). The PV Asia Pacific Conference 2012 was jointly organised by SERIS and the Asian Photovoltaic Industry Association (APVIA)

Keywords: CIGS; CZTS; Mo back contact; RF magnetron sputtering; resistivity; RF power

* Corresponding author. Tel.: +603-8921-6325; fax: +603-8921-6146.
E-mail address: nowshad@eng.ukm.my

1876-6102 © 2013 The Authors. Published by Elsevier Ltd. Open access under CC BY-NC-ND license.
Selection and peer-review under responsibility of Solar Energy Research Institute of Singapore (SERIS) – National University of Singapore (NUS). The PV Asia Pacific Conference 2012 was jointly organised by SERIS and the Asian Photovoltaic Industry Association (APVIA)
doi:10.1016/j.egypro.2013.05.057

1. Introduction

Renewable energy is one of the most favourable choices to meet the energy demand throughout the world. Thin film solar cell technology is one of the most promising candidates to solve the upcoming energy crisis. Moreover it is a faster fabrication process in comparison with traditional silicon wafer based solar cell technology [1-5]. Among them CdTe and CIGS are the most favourable choices. World first large scale PV industrial production was by CdTe at the lowest cost of USD 0.75/W_p with module efficiency of 11% [1, 6]. Although the highest efficiency in case of CdTe base solar cell is 18.3% [7]. The highest efficiency of CIGS based solar cell is 20.4% [2]. However the overall module efficiency is 13% with the cost of USD 1.2/W_p, which is certainly higher than CdTe base solar cell [8]. Here, the overall module efficiencies of the two technologies are very close, giving CdTe cells the advantage of lower production cost. Nevertheless the quality of the substrate, deposition conditions as well as appropriate back contact is still a matter of issue. Among several material for back contact, Molybdenum is one of the most appropriate material because of its high conductivity as well as inertness [3-5]. It is believed that smoother surface can produce more uniform growth, less pin holes, better crystallinity as well as less shunting [5]. RF magnetron is one of the most leading deposition processes. Moreover the properties of sputter-deposited Mo thin films can be controlled by sputtering parameters such as RF power, pressure and temperature [9, 10]. In this work we have investigated the influence of various sputtering process parameters on the electrical, structural, and morphological of Mo thin films on soda lime glass (SLG) and molybdenum (Mo) sheet substrates.

2. Experimental work

Thin Mo sheets and soda lime glass (SLG) were cleaned in a ultrasonic bath using 4-stage methanol-acetone-methanol-DI water recipe for 10 minutes in each stage, followed by nitrogen gas drying. Mo target (99.95% purity) was pre-sputtered for between 10-15 minutes in order to remove any oxide on the surface. RF sputtering was carried out on Mo sheet and SLG at various RF power, operating pressure and temperature. The overall process parameters are shown in Table 1 below. A time limit of 35 to 70 minutes was maintained and thickness of 250 nm to 300 nm was found from SEM cross sectional images. Using XRD, SEM, AFM and Hall measurement the films were characterised and their possible effects on solar cell fabrication were investigated.

Table 1. List of the deposition parameters and corresponding variation ranges, used to deposit the Mo thin films on Mo sheet and SLG

Parameters	Variation range
RF power (W)	60,80,100,120
Operating pressure (mTorr)	8.5,10,15,20
Operating temperature (˚C)	80,100,150,200
Base pressure (Torr)	$8x10^{-5}$
Deposition time (minute)	35-70
Thickness (nm)	250-300

3. Result and discussion

From the SEM image presented in Fig. 1, we compare the surface morphology of the Mo sputtered on Mo sheet and soda lime glass (SLG) at various powers. It is readily observed that as the RF power increased more uniform coverage has been found on top of both Mo sheet and soda lime glass. During low RF power deposition process, the ejected Mo particles have lower energy to re-crystallise, which can

cause loose and porous Mo film to be formed [10]. On the contrary as the power increased, Mo particles have higher energy and as a result films with more uniform surface are grown on both Mo sheet and soda lime glass. The variation of RF power has a significant impact on surface roughness as listed in Table 2 and graphed in Fig. 2. As the power increases the kinetic energy of the Mo particles increases [10-12] and bombardment of high kinetic energy particles on both Mo sheet and SLG can possibly induce higher surface roughness. Moreover, as the kinetic energy of the Mo particles increase, the vibration of Mo particles on surface also increases and this also can cause higher surface roughness. From Fig. 2 it is shown that Mo deposited on Mo sheet exhibit higher roughness compare to SLG, due to Mo sheet itself rougher than SLG. The roughness index was found to be in the range of 0.0027 nm-6.012 nm in case of Mo sheet and 0.0022 nm-5.048 nm in case of SLG. Figure 3 shows the XRD patterns for Mo films deposited on Mo sheet and SLG. The XRD pattern for all films indicated the most intense peak at $2\theta=58.6^\circ$ and $2\theta=73.64^\circ$ correspond to <200> and <211> preferred orientation of BCC structure in case of Mo films deposited on Mo sheet. On the other hand $2\theta=39.96^\circ$ Correspond to <110> preferred orientation of BCC structure in case of Mo films on SLG. The ratio of peak intensity I_{200}/I_{211} was calculated in case of Mo films deposited Mo sheet. It was found that as the RF power increased the ratio of peak intensity decreases as listed in Table 2 and shown in Fig. 3. This indicates that the Mo growth tends to have two major crystal orientations as the RF power increases. However in case of Mo deposited on SLG peak intensity on top of SLG was almost same at different power levels. The dependency of the electrical properties are listed in Table 3 and shown in Fig. 4. From Fig. 4 it can be observed that resistivity is inversely proportional to the RF power. As the power increases, resistivity decreases in both cases Mo film deposited on Mo sheet and SLG. At lower power Mo particles do not contain sufficient energy to recrystallise the Mo films at the surface of the substrate. As a result the formation of Mo film become loose and porous when RF power is lower and cause higher resistivity [10]. In case of Mo film deposited on Mo sheet, resistivity decreases from 8.25×10^{-9} Ω.m to 2.43×10^{-9} Ω.m as the RF power increases from 60 W to 120 W. However, resistivity drastically decreases from 5×10^{-5} Ω.m to 6.65×10^{-6} Ω.m in case of Mo films deposited on SLG. Moreover as seen in Fig. 4 mobility is inversely proportional to bulk concentration. In the case of Mo films deposited on Mo sheet, as the power increases bulk concentration increases slightly at the beginning then decreases again at the power level of 100 W. However at higher power level of 120 W, bulk concentration increases significantly up to 3.69×10^{23} cm^{-3}, which causes lower mobility of 6.95×10^{3} cm^2/Vs. On the contrary Mo film deposited on SLG exhibits opposite result as shown in Fig. 4. As the RF power increases at first bulk concentration increases, however at higher power of 120 W bulk concentration decreases up to 3.57×10^{19} cm^{-3}. As a result, although mobility decreases at the beginning, however at higher power level mobility increases significantly up to 2.56×10^{4} cm^2/Vs.

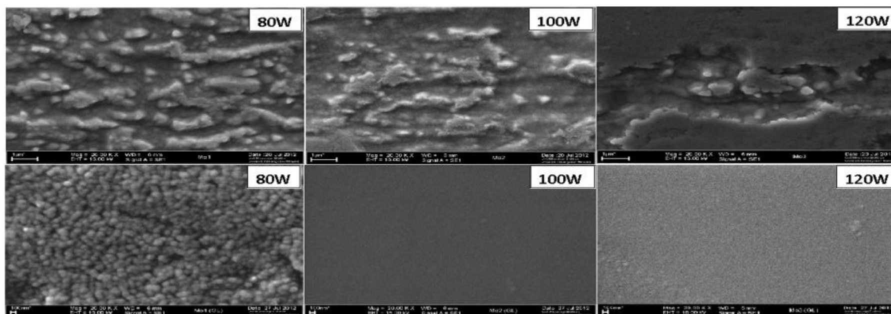

Fig. 1. Surface morphology of Mo films deposited on Mo sheet (top row) and SLG (bottom row) at various RF power, while operating pressure of 10 mTorr and deposition temperature of 100˚C remained constant.

Table 2. List of surface roughness (RMS value) of Mo films on Mo sheet and SLG as well as I_{200}/I_{211} on Mo sheet deposited at various RF power.

RF Power (W)	Surface Roughness(nm) on Mo sheet	I_{200}/I_{211} (Mo sheet)	Surface Roughness(nm) on SLG
60	0.027585	17.53	0.002272
80	3.0154	17.11	1.22356
100	3.5324	16.88	1.892
120	6.012	1.92	5.0489

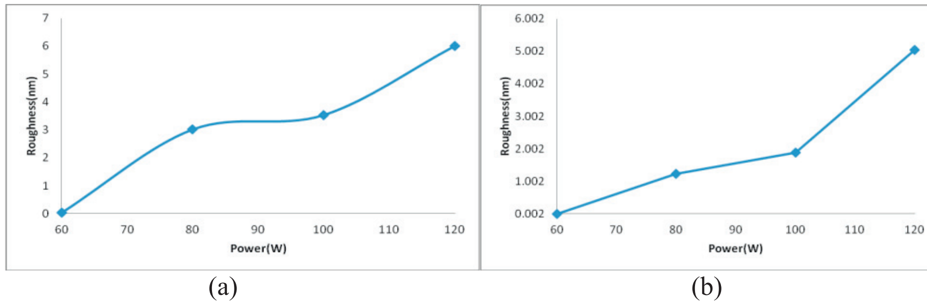

Fig. 2. Variation of the surface roughness of Mo films (a) On Mo sheet and (b) On SLG, in dependence on RF power

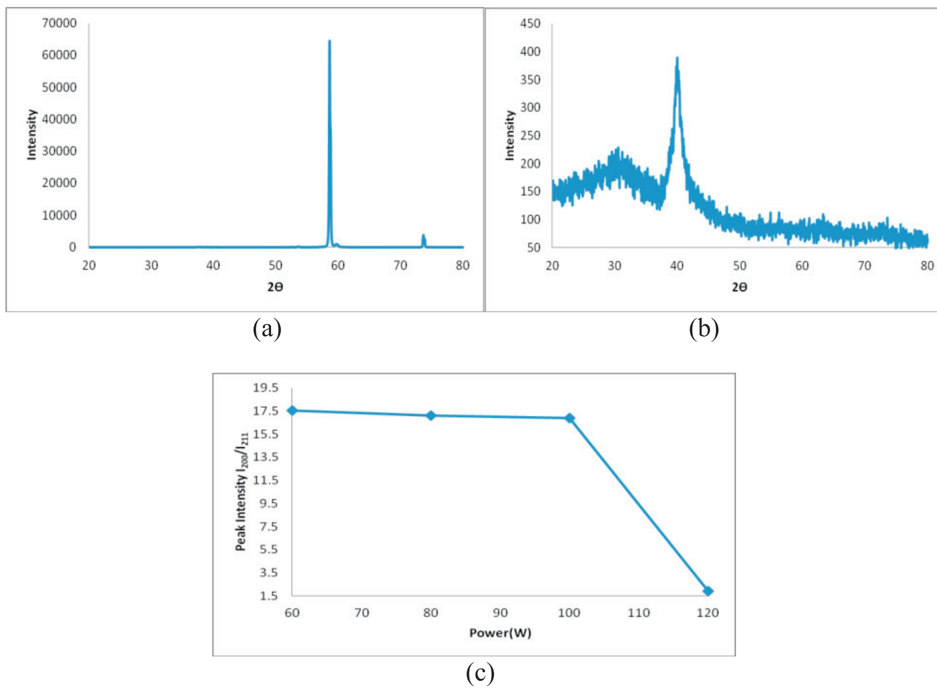

Fig. 3. XRD spectra of the Mo films sputtered with different powers: (a) Mo films on Mo sheet, (b) Mo films on SLG, and (c) Variation of peak intensity of Mo films on Mo sheet.

Table 3. Effect of various RF power on electrical properties of Mo films deposited on (a) Mo sheet and (b) SLG.

	(a)			(b)		
RF Power (W)	Resistivity (Ω)	Bulk Concentration (cm^{-3})	Mobility (cm^2/V.s)	Resistivity (Ω.m)	Bulk Concentration (cm^{-3})	Mobility (cm^2/V.s)
60	$8.25x10^{-9}$	$9.24x10^{21}$	$8.19x10^{4}$	$5x10^{-5}$	$2.27x10^{20}$	$5.50x10^{2}$
80	$4.09x10^{-9}$	$6.02x10^{22}$	$2.54x10^{4}$	$2.95x10^{-5}$	$5.24x10^{20}$	$4.04x10^{2}$
100	$3.34x10^{-9}$	$4.72x10^{21}$	$3.97x10^{5}$	$2.85x10^{-5}$	$6.19x10^{20}$	$3.54x10^{2}$
120	$2.43x10^{-9}$	$3.69x10^{23}$	$6.95x10^{3}$	$6.65x10^{-6}$	$3.67x10^{19}$	$2.56x10^{4}$

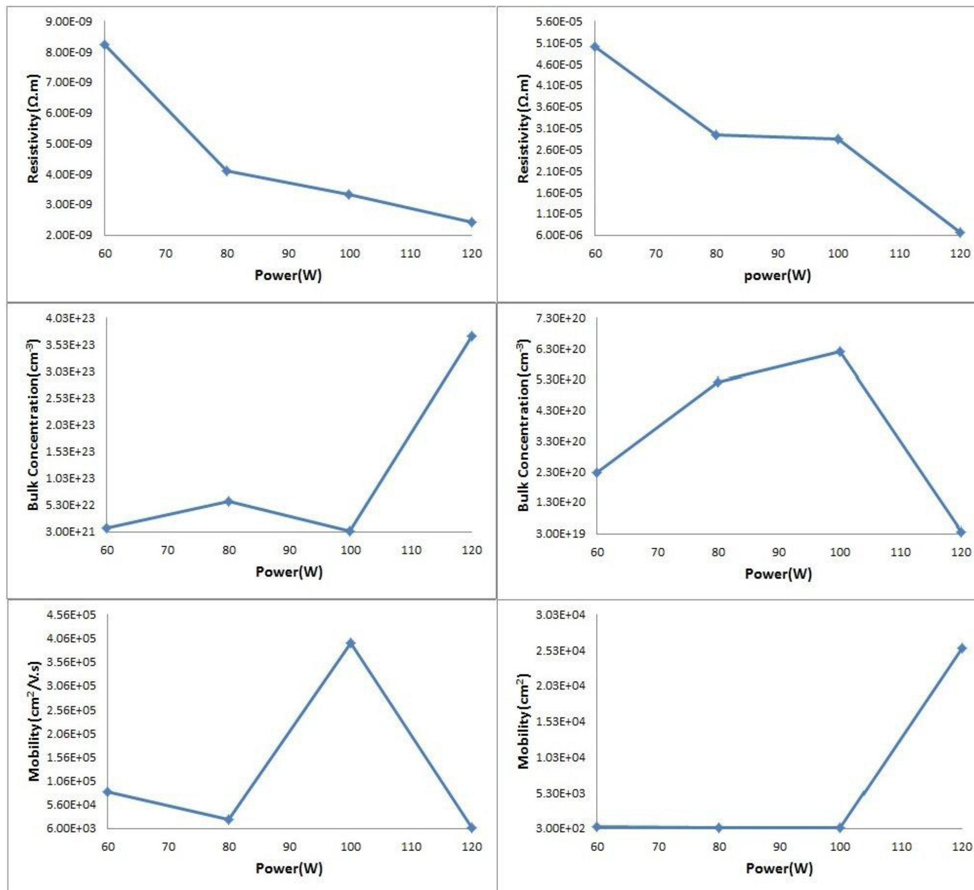

Fig. 4. Resistivity, bulk concentration and mobility of Mo films deposited on Mo sheet (left column) and SLG (right column) at various RF power.

Figure 5 exhibits the comparison of surface morphology under different operating pressure level. Increase in operating pressure produces films which are more uniform with smoother surface morphology. Better surface morphology was found on top of soda lime glass rather than Mo sheet. Figure 6 depicts AFM results of Mo films on Mo sheet and Mo films on SLG. Surface roughness is highly depends upon the operating pressure as charted in Table 4 and shown in Fig. 6. It is clear from the Fig. 6 that as the pressure increases the roughness decreases in both case of Mo sheet and SLG. This attributes

to the fact that at higher pressure the Mo particles contain lower energy and hit the surface with lower energy as a result lower roughness. However at the highest pressure of 20 mTorr the roughness tends to increase again in both case of Mo deposited on Mo sheet and SLG. Hence roughness on SLG is lesser than Mo sheet as predicted. Here, XRD patterns have similar peak as previous. The variation of peak intensity due to various operating pressure are listed in Table 4 and showed in Fig. 7. As shown in Fig. 7 the ratio of peak intensity I_{200}/I_{211} decreased at first in case of Mo films deposited on Mo sheet, however up to 15 mTorr pressure it increased again which indicate Mo growth at single preferential orientation. Nevertheless, at high pressure of 20 mTorr the ratio decreases again, which indicates the growth of Mo film contains two major crystal orientations. On the other hand on top of SLG peak intensity was almost same as the pressure increases. The effect of different working pressure on electrical properties are listed in Table 5 and graphed in Fig. 8. From Fig. 8, it is clear that resistivity has a proportional relation to working pressure. As the working pressure increases resistivity increases in both cases of Mo films deposited on Mo sheet as well as SLG. This attributes to the fact that at lower working pressure incident atoms contain higher energy because of lesser scattering. These energetic incident atoms impart higher momentum to those Mo particles and help to fill up micro voids and vacancies. As a result, better crystallinity and larger grain growth are observed [11]. However at higher working pressure incident Mo particles have lower and momentum. As a result, crystallinity and grain growth both degrade resulting in higher resistivity. In case of Mo film deposited on Mo sheet resistivity increases from 1.31×10^{-9} Ω.m to 9.47×10^{-9} Ω.m as the working pressure increases from 8.5 mTorr to 20 mTorr. On the other hand, resistivity considerably increases from 2.88×10^{-5} Ω.m to 1.88×10^{-3} Ω.m in case of Mo films deposited on SLG. As shown in Fig. 8, bulk concentration and mobility are inversely proportional in both cases of Mo films deposited on Mo sheet and SLG. In case of Mo films deposited on Mo sheet bulk concentration decreases from 1.28×10^{23} cm^{-3} to 1.04×10^{22} cm^{-3} as the working pressure increases up to 15 mTorr. As a result, though mobility decreases at working pressure of 10 mTorr from 3.72×10^{4} cm^{2} to 2.54×10^{4} cm^{2}, but at working pressure 15 mTorr it increases up to 8.08×10^{4} cm^{2}. Nevertheless at higher working pressure of 20 mTorr bulk concentration increases, this causes the mobility to decrease. Then again in case of Mo films deposited on SLG bulk concentration shows some random result as shown in Table 5 and Fig. 8. As working pressure increases bulk concentration increases as depict in Table 5, however again decreases at working pressure of 15 mTorr and finally at higher working pressure of 20 mTorr increases up to 1.22×10^{22} cm^{-3}. On the contrary mobility exhibits opposite result of bulk concentration and finally decreases up to 1.88×10^{-3} cm^{2}.

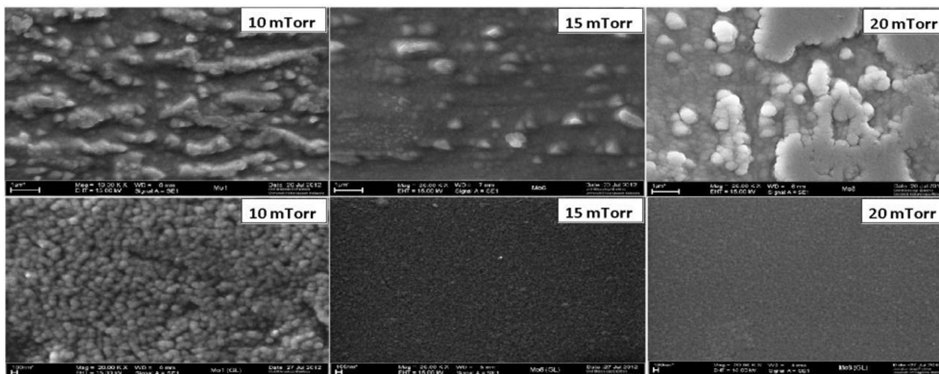

Fig. 5. Surface morphology of Mo films deposited on Mo sheet (top row) and SLG (bottom row) at various operating pressure, where RF power of 80W and deposition temperature of 100˚C remained constant.

Table 4. List of surface roughness (RMS value) of Mo films on Mo sheet and SLG as well as I_{200}/I_{211} on Mo sheet deposited at various operating pressure.

Operating Pressure (mTorr)	Surface Roughness(nm) on Mo sheet	I_{200}/I_{211} (Mo sheet)	Surface Roughness(nm) on SLG
8.5	19.323	17.42	1.49669
10	4.98836	17.13	1.22356
15	2.34058	20.766	1.02453
20	5.06985	16.15	2.02654

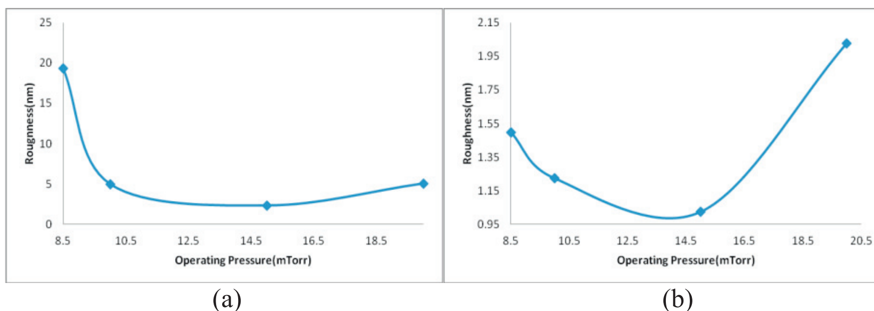

(a) (b)

Fig. 6. Variation of the surface roughness of Mo films (a) On Mo sheet and (b) On SLG, in dependence on operating pressure.

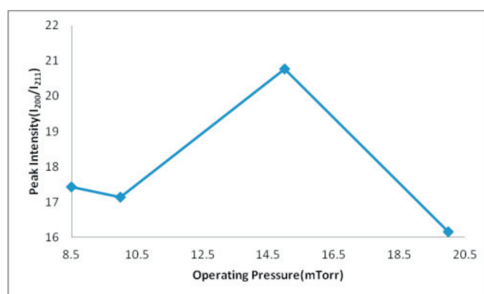

Fig. 7. Variation of peak intensity of Mo films deposited on Mo sheet at various operating pressure.

Table 5. Effect of various operating pressure on electrical properties of Mo films deposited on (a) Mo sheet and (b) SLG.

	(a)			(b)		
Operating Pressure (mTorr)	Resistivity (Ω)	Bulk Concentration (cm^{-3})	Mobility (cm^2/V.s)	Resistivity (Ω.m)	Bulk Concentration (cm^{-3})	Mobility (cm^2/V.s)
8.5	$1.31x10^{-9}$	$1.28x10^{23}$	$3.72x10^{4}$	$2.88x10^{-5}$	$9.75x10^{19}$	$2.22x10^{3}$
10	$4.09x10^{-9}$	$6.02x10^{22}$	$2.54x10^{4}$	$2.95x10^{-5}$	$5.24x10^{20}$	$4.04x10^{2}$
15	$7.43x10^{-9}$	$1.04x10^{22}$	$8.06x10^{4}$	$2.09x10^{-4}$	$5.64x10^{19}$	$5.31x10^{2}$
20	$9.47x10^{-9}$	$2.02x10^{22}$	$3.26x10^{4}$	$1.88x10^{-3}$	$1.22x10^{20}$	$2.74x10^{1}$

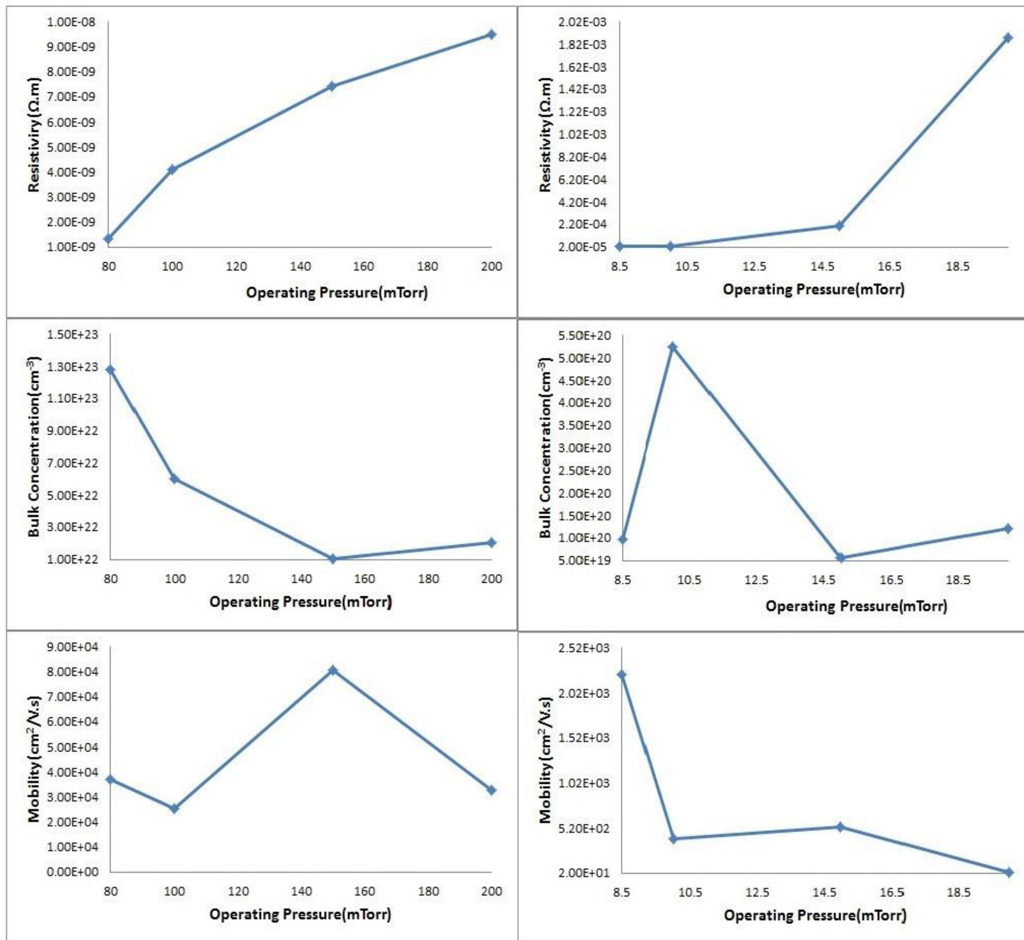

Fig. 8. Resistivity, bulk concentration and mobility of Mo films deposited on Mo sheet (left column) and SLG (right column) at various growth pressure.

Figure 9 represents the comparison under different deposition temperature. Here, at first uniform coverage has been obtained on top of Mo sheet as the deposition temperature increases. However at higher deposition temperature (>150 ˚C) the surface becomes rough again on top of Mo sheet. In case of soda lime glass smother surface morphology is observed as the deposition temperature increases. It was found that roughness has a proportional relation with deposition temperature. The influence of the variation of deposition temperature on roughness is listed in Table 6 and graphed in Fig. 10. From Fig. 10 it can be seen that roughness is proportionally related to deposition temperature in the case of Mo films deposited on Mo sheet. On the contrary, in the case of Mo films deposited on SLG increases although at the beginning roughness decreases as the deposition temperature however, at deposition temperature greater than 100˚C roughness increases again, as shown in Fig. 10. This is simply because as deposition temperature increases the kinetic energy of the Mo particle increases, consequently those particles strike the surface with high kinetic energy which causes higher roughness. Here also similar XRD pattern was observed as previous at various deposition temperatures. The deposition temperature has a significant effect on peak intensity ratio I_{200}/I_{211} in case of Mo film deposited on Mo sheet, as listed in Table 6 and

graphed in Fig.11. Hence as the deposition temperature increases the peak intensity ratio decreases as shown in Fig. 11. Which indicates that the Mo film have two major crystal orientation as the temperature increases. However at higher deposition temperature of 200˚C the ratio increases dramatically, which indicates that the presence single crystal orientation. Then again no significant variation of crystallographic orientation was observed in case of Mo film deposited on SLG. The dependency of the electrical properties on deposition temperature are listed in Table 7 and graphed in Fig. 12. From Fig. 12 it can be depicted that resistivity is inversely proportional to deposition temperature in both cases of Mo films deposited on Mo sheet as well as SLG. At lower deposition temperature Mo particle contains lower energy and this result in loose and porous Mo films of reduced crystallinity and grain growth, while resistivity increases. However at higher deposition temperature Mo particles contain higher energy, which help to fill up the micro voids or vacancies resulting in enhance grain growth and better crystallinity. At the same time as this helps to decrease resistivity. In case of Mo film deposited on Mo sheet resistivity decreases from 8×10^{-9} Ω.m to 1.2×10^{-9} Ω.m as the operating temperature increases from 80 ˚C to 200 ˚C. On the other hand in case of Mo films deposited on SLG resistivity decreases from 4.61×10^{-5} Ω.m to 2.2×10^{-5} Ω.m. Due to variation of deposition temperature bulk concentration varies from 4.55×10^{22} cm^{-3} to 3.99×10^{22} cm^{-3} in case of Mo films deposited on Mo sheet as listed in Table 7. Mobility is proportionally related to deposition temperature as graphed in Fig. 12. As the deposition temperature increases mobility increases from 1.72×10^{4} cm^2/Vs to 1.31×10^{5} cm^2/Vs. Moreover this increased mobility resulting in reduced resistivity. In case of Mo film deposited on SLG bulk concentration is inversely proportional to mobility. Due to the variation of deposition temperature at the beginning bulk concentration increases from 1.02×10^{20} cm^{-3} to 5.24×10^{20} cm^{-3} until 100˚C. It causes the mobility to decrease from 2.22×10^{3} cm^2/Vs to 4.04×10^{2} cm^2/Vs. Then again until 200˚C bulk concentration decreases to 1.35×10^{20} cm^{-3}, resulting in enhanced mobility of 2.1×10^{3} cm^2/Vs.

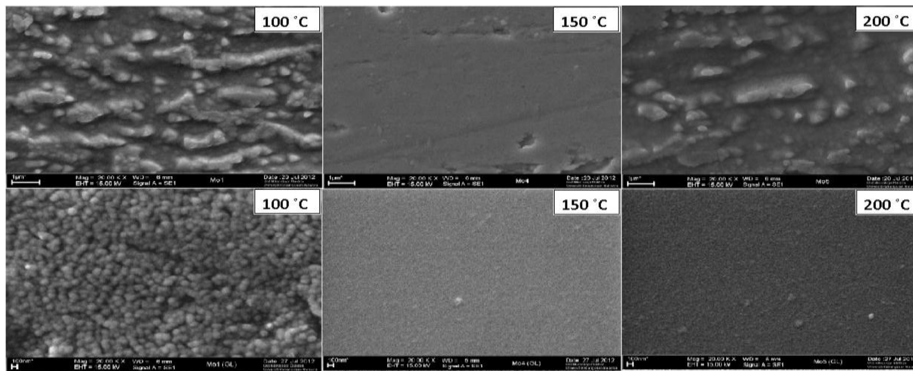

Fig. 9. Surface morphology of Mo films deposited on Mo sheet (top row) and SLG (bottom row) at various depositions temperature, where RF power of 80W and operating pressure of 10 mTorr remained constant.

Table 6. Surface roughness (RMS value) of Mo films on Mo sheet and SLG on Mo sheet deposited at various deposition temperature.

Deposition Temperature (˚C)	Surface Roughness(nm) on Mo sheet	I_{200}/I_{211} (Mo sheet)	Surface Roughness(nm) on SLG
80	0.017086	20.29	4.82205
100	4.98836	17.13	1.10681
150	5.2325	3.48	1.31168
200	7.40839	25.31	1.90201

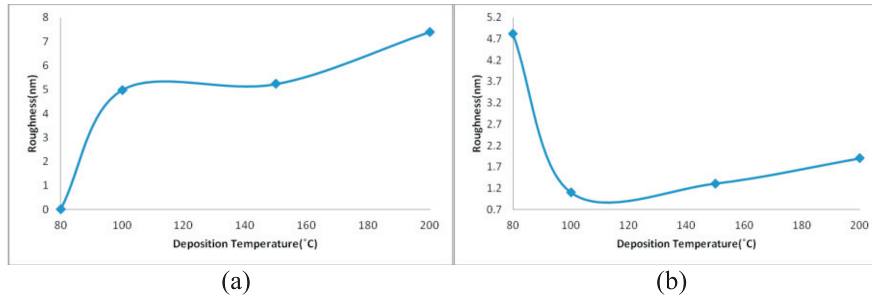

(a) (b)

Fig. 10. Variation of the surface roughness of Mo films (a) on Mo sheet and (b) on SLG, in dependence on deposition temperature.

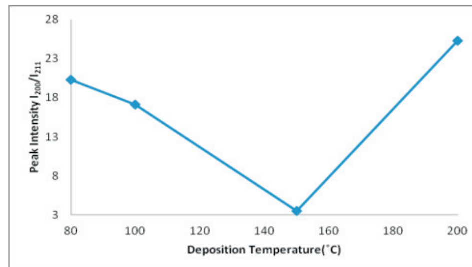

Fig. 11. Variation of peak intensity of Mo films deposited on Mo sheet at various deposition temperatures.

Table 7. Effect of various operating pressures on electrical properties of Mo films deposited on (a) Mo sheet and (b) SLG.

Deposition Temperature (˚C)	Resistivity (Ω.m) (Mo sheet)	Bulk Concentration (cm^{-3}) (Mo sheet)	Mobility (cm^2/V.s) (Mo sheet)	Resistivity (Ω) (SLG)	Bulk Concentration (cm^{-3}) (SLG)	Mobility (cm^2/V.s) (SLG)
80	$8.00x10^{-9}$	$4.55x10^{22}$	$1.72x10^{4}$	$4.61x10^{-5}$	$1.02x10^{20}$	$1.33x10^{3}$
100	$4.09x10^{-9}$	$6.02x10^{22}$	$2.54x10^{4}$	$2.95x10^{-5}$	$5.24x10^{20}$	$4.04x10^{2}$
150	$3.87x10^{-9}$	$2.19x10^{22}$	$7.36x10^{4}$	$2.73x10^{-5}$	$4.13x10^{20}$	$5.54x10^{2}$
200	$1.20x10^{-9}$	$3.99x10^{22}$	$1.31x10^{5}$	$2.20x10^{-5}$	$1.35x10^{20}$	$2.10x10^{3}$

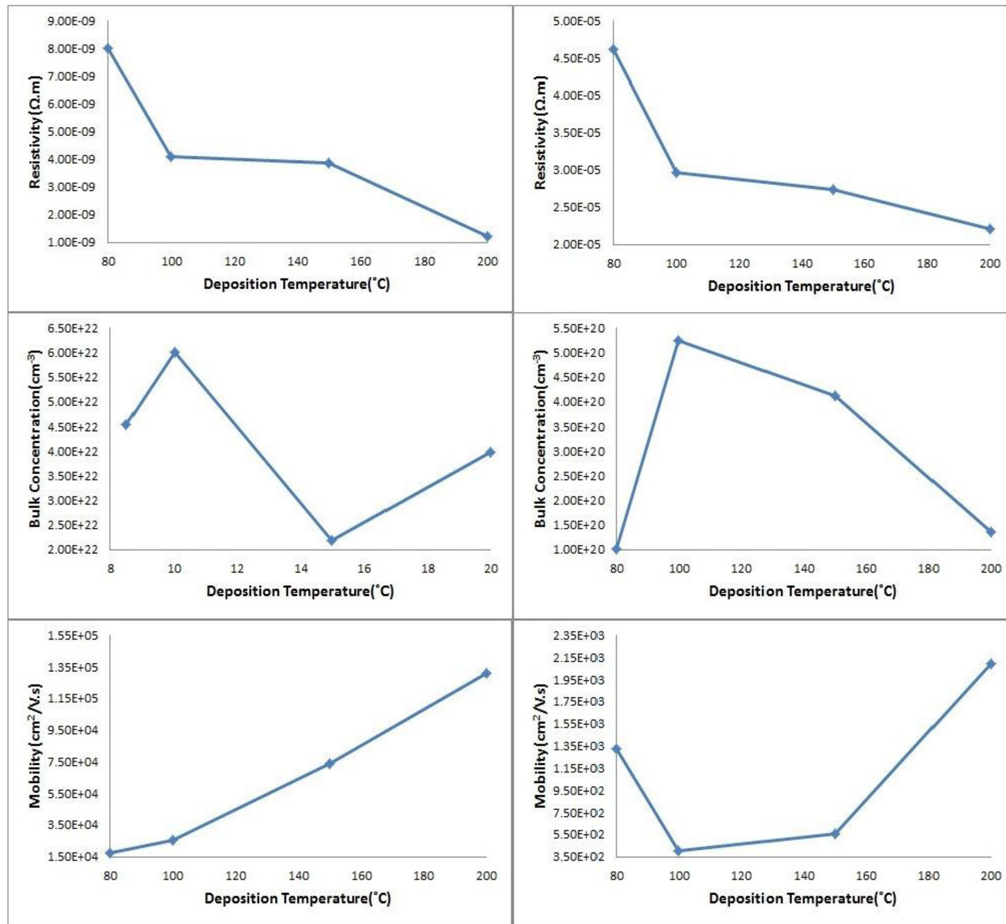

Fig. 12. Resistivity, bulk concentration and mobility of Mo films deposited on Mo sheet (left column) and SLG (right column) at various deposition temperatures.

The crystallite size was calculated using Scherrer equation which is given by [13].

$$\text{Crystallite size, } D = 0.89\, \lambda / \beta \cos\theta \quad (1)$$

Where D is the main grain (crystallite) size, λ is X-ray wavelength which is 1.54Å. β is the FWHM measured in radians and θ is Bragg angle. Grain size of 315.08Å and 379.42Å was found in case of Mo films on Mo sheet and SLG. However from Scanning Electron Microscope (SEM), the grain size of 178.6 nm – 669.9 nm was found in both cases of Mo films deposited on Mo sheet and SLG. It can be noticed that there is certain discrepancy between the grain sizes by two different processes. It might be due to the fact that the grain size measured by XRD is for very uniform films with same crystallite size, which is not the case here as found from SEM.

4. Conclusion

In this study, we analyzed the effect of sputtering power, operating pressure and deposition temperature on the properties of Mo thin films grown on Mo sheet and SLG. The electrical and structural properties are highly influenced by the deposition parameters. At higher RF power and operating pressure better surface morphology was found. Grain size of 315.08 Å to 379.42 Å from XRD and 178.6 nm to 669.9 nm from SEM was found in both cases. Resistivity of RF-sputtered Mo films is highly dependent on sputtering process variable. Lowest resistivity of 1.2×10^{-9} Ω.m was found in case of Mo film deposited on Mo sheet and the corresponding deposition conditions are 80 W, 200 ˚C and 10 mTorr. On the other hand, on top of SLG lowest resistivity of 6.65×10^{-6} Ω.m is obtained at the deposition condition of 120 W, 100˚C and 10 mTorr. The electrical resistivity is mainly attributed to the higher mobility, lower roughness and low bulk concentration.

Acknowledgements

The authors would like to acknowledge and appreciate the contribution of the Ministry of Higher Education of Malaysia (MOHE) through its research grant with code FRGS/1/2011/TK/UKM/01/20. Appreciations are also extended to Solar Energy Research Institute (SERI), Universiti Kebangsaan Malaysia and the Department of Electrical Electronic and Systems Engineering of Universiti Kebangsaan Malaysia (UKM).

References

[1] First Solar, Inc. Announces Fourth Quarter and Year-end 2010 Financial Results http://investor.firstsolar.com/phoenix.zhtml?c=201491&p=irolnewsArticle& ID=1532742

[2] New CIGS Solar Cell Efficiency Record, January 24, 2013 http://pv-tech.org/news/empa_achieves_record_efficiency_for_converting_sunlight_into_electricity?utm_source=PV-Tech&utm_campaign=19182a86cd-PV_Tech_Thin_Film_Newsletter_24_January_2013&utm_medium=email

[3] Singh VP, McClure JC, Lush GB, Wang W, Wang X, Thompson GW, Clark E.Thin film CdTe-CdS hetero-junction solar cells on lightweight metal substrates. *Solar Energy Materials Solar Cells* 1999;**59**: 145-61.

[4] Hodges DR. Development of CdTe thin film solar cells on flexible foil substrates, *PhD Thesis*, University of South Florida, 2009.

[5] Drayton J, Vasko A, Gupta A, Compaan AD. Magnetron sputtered CdTe solar cells on flexible substrates. *Proc. 31st IEEE Photovoltaic Specialists Conf., Florida, USA;* 2005, pp. 406- 409.

[6] Q-Cells Sets CIGS 13.0% Efficiency Record 11 June, 2010 www.renewableenergyworld.com/reabanners/www/delivery/ck.php?n=917509c

[7] PV Efficiency Record http://www.greentechmedia.com/articles/read/GE-Research-Beats-First-Solars-CdTe-PV-Efficiency-Record

[8] McCabe, J. Metrics for thin film solar CIGS company comparisons. *Solar Industry Veteran* July 26, 2010 http://www.renewableenergyworld.com/rea/news/article/2010/07/metrics-for-thin-film-solar-cigs-company-comparisons.

[9] Scofield JH, Duda A, Albin D, Ballard BL, Predecki PK. Sputtered molybde- num bilayer back contact for CIS basedpolycrystalline thin-film solar cells. *Thin Solid Films* 1995; **260**:26-31.

[10] Li ZH, Cho ES, Kwon SJ. Molybdenum thin film deposited by in-line DC magnetron sputtering as a back contact forCu(In,Ga)Se2 solar cells. *Applied Surface Science* 2011; **257**: 9682-8.

[11] Pethe SA, Takahashi E, Kaul A, Dhere NG. Effect of sputtering process parameters on film properties of molybdenum back contact. *Solar Energy Materials & Solar Cells* 2012;**100**: 1-5.

[12] Scofield JH, Duda A, Albin D, Ballardb BL, Predeckib PK. Sputtered molybdenum bilayer back contact for copper indium diselenide-based polycrystalline thin-film solar cells. *Thin Solid Films* 1995;**260**: 26-31.

[13] Kaeble EF. Handbook of X-rays, McGraw-Hill, NY, USA, 1967.